

Flash STU: Fast Spectral Transform Units

Y. Isabel Liu*
Princeton University

Windsor Nguyen*
Princeton University

Yagiz Devre
Princeton University

Evan Dogariu
Princeton University / NYU †

Anirudha Majumdar
Princeton University

Elad Hazan
Princeton University ‡

September 17, 2024

Abstract

This paper describes an efficient, open source PyTorch implementation¹ of the Spectral Transform Unit [1]. We investigate sequence prediction tasks over several modalities including language, robotics, and simulated dynamical systems. We find that for the same parameter count, the STU and its variants outperform the Transformer as well as other leading state space models across various modalities.

1 Introduction

The Spectral Transform Unit was recently proposed in [1] based on the spectral filtering technique of [16]. This neural network architectural unit is motivated by state space models for linear dynamical systems. The key innovation of spectral state space models lies in their use of fixed convolutional filters which do not require learning. This structure offers significant robustness in theory as the performance of the model is not influenced by the spectrum of the underlying dynamics nor the dimensionality of the problem, making it suitable for tasks that require long-term memory.

In this paper we describe an open source PyTorch implementation of the STU and experiments as well as ablation studies to understand its properties. We study several sequence prediction problems across various modalities, including synthetic time series generated from linear dynamical systems, robotics control sequences, and natural language sequences.

1.1 Description of the Spectral Transform Unit

In the STU architecture, the schematic of which is given in Figure 1, the output is generated as a transformation of the input sequence that involves (optional) lifting of the input dimension by a learned transformation to a higher dimension, convolution with a set of fixed filters (i.e. spectral filtering), projection with a set of learned parameters, and (optional) learned nonlinearities. We can thus write

$$\hat{y}_t = \sigma \left(\sum_{i=1}^k M_i \cdot \langle \Phi_i, u_{t:t-L} \rangle \right),$$

where M_i are fixed projections, σ is a nonlinearity, and $\Phi_{1:k}$ are k fixed filters that can be computed a-priori, and for simplicity we don't explicitly write the lifting in the mathematical expression. The filters $\Phi_{1:k}$ are the eigenvectors

*Equal contribution. Order determined alphabetically by last name.

†ed2719@nyu.edu

‡isabel.liu, minhtringuyen, yagiz.devre, ani.majumdar, ehazan,@princeton.edu

¹<https://github.com/windsornguyen/flash-stu/>

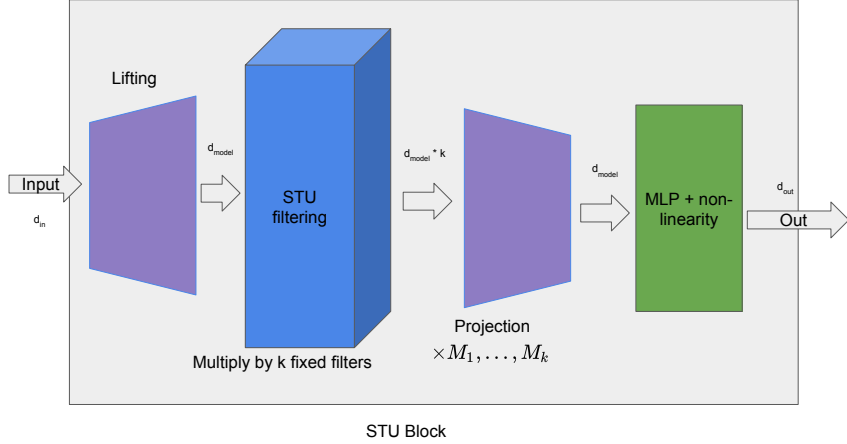


Figure 1: The basic architecture of the Spectral Transformer Unit

corresponding to the largest eigenvalues of the positive semidefinite matrix given by the outer products of all impulse response vectors of a given length L .²

$$Z = \int_{\alpha=0}^1 \mu_{\alpha} \mu_{\alpha}^{\top} d\alpha, \quad \mu_{\alpha} = (1, \alpha, \dots, \alpha^L).$$

These filters can be computer a-priori and stored before the actual sequence is observed.

An important speedup due to [1] is called the *tensordot approximation*, or **STU-T**, whereby the tensors M_i are approximated as a tensor of two matrices. In more detail, if d_{in} is the dimension of the input token embeddings, and d_{out} of the output dimensions, then the tensors M_i have dimensionality $d_{in} \times k \times d_{out}$.

The tensordot approximation decomposes each M_i as a product of $M_i^1 \times M_i^2$ with dimensions $M_i^1 \in \mathbb{R}^{d_{model} \times k}$, $M_i^2 \in \mathbb{R}^{d_{model} \times d_{out}}$, where k is the number of filters. This allows us to perform the projection before the convolution operation, and reduce the computational complexity by approximately a factor of k . However, the approximation reduces the expressivity of the model, and the theoretic results on the learnability of marginally stable linear dynamical systems do not trivially apply. In practice, its performance is competitive, and the computational advantage is significant.

2 Experiments with synthetic data

We begin our investigation of STU phenomena with some simple yet representative synthetic tasks that have become commonplace in the sequence modeling literature. In particular, we aim to understand the behavior of the STU in environments with long memory and nonlinearities, especially as we introduce feed-forward layers and deeper architectures. We compare against S4 [14], a standard SSM architecture, as well as the vanilla transformer layer [33].

2.1 Linear dynamical systems

In a linear dynamical system (LDS) the outputs $\{y_t\}$ of a sequence are generated according to the dynamics equations

$$x_{t+1} = Ax_t + Bu_t, \quad y_t = Cx_t + Du_t,$$

²More precisely, there could be more multipliers to the matrix of the form $(1 - \alpha)$ or $(1 - \alpha^2)$, depending on the precise variant, see [16, 1, 15].

where $\{u_t\}$ is an (observed) input sequence and $\{x_t\}$ are hidden states of the system. The matrices A, B, C, D are called "system matrices" and are unknown to the sequence predictor. Typical approaches to learning in this setting scale in complexity with hidden state dimension d_{hidden} and effective system memory $1/\delta$, where $\rho(A) = 1 - \delta$ is the spectral radius of A . For an in-depth treatment of linear dynamical systems as well as methods to learn and predict them, see the text [15].

The task of sequence prediction in this case is to predict \hat{y}_{t+1} given all the previous inputs and outputs $u_{1:t}, y_{1:t}$ and to minimize the loss vs. the actual output y_{t+1} . We evaluate the mean squared error of the STU’s predictions vs. other methods where the sequence was generated by a linear dynamical system.

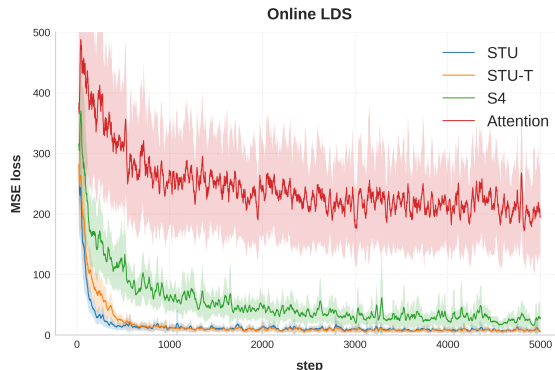


Figure 2: Mean squared error $\|\hat{y}_{t+1} - y_{t+1}\|^2$ of the different layers on a single sequence from an LDS

Experiment details and conclusions. We apply random inputs to linear dynamical systems with random system matrices with $d_{\text{input}} = d_{\text{output}} = 5$ and hidden state dimension $d_{\text{hidden}} = 256$. The transition matrix A is symmetrized and normalized so that $\rho(A) = 0.99$ to give the system an effective memory of ≈ 100 , which is what we set the context length to. Such a setting has the properties of (1) long memory and (2) a large hidden state, which we believe to be major sources of complexity in real-world applications.

We compare against a standard attention layer, with 8 heads and the ALiBi [25] positional embedding, and a diagonal S4 layer [14] with hidden dimension equal to d_{hidden} . All layers have a width of 32 and are trained for 5,000 steps with the RMSProp optimizer. Results are plotted in Figure 2 with error bars over 16 trials.

We see that both the vanilla STU and its approximate version STU-T are able to reliably achieve small loss in this setting with quick and robust convergence, while the performances of the other methods vary across random seeds. Note that the width of the STU layer does not need to be as large as d_{hidden} to perfectly capture the dynamics, which is consistent with theory. Furthermore, the STU-T approximation is able to roughly match vanilla STU’s performance even on these multi-input multi-output (MIMO) systems. This experiment confirms that the STU layer is a powerful and robust SSM primitive.

2.2 Optimization behavior

We saw on the linear dynamical system that the STU layers seem to have a comparatively easier time optimizing. This is expected since a single STU layer under MSE loss is a convex parameterization, whereas the losses of an S4 and an attention model are nonconvex³. Following [20], we choose two random directions in the high-dimensional space, move along these directions by varying amounts x_{step} and y_{step} , compute the loss of the model with perturbed parameters for each coordinate pair in these directions, and plot the loss values as heights on a 2D grid. By doing this,

³For S4, Mamba [13], and any other model that parameterizes an LDS directly, this nonconvexity even grows with sequence length.

we are able to get a sense for the local geometry of a reduced-dimension loss landscape.

Figures 3-5 visualize these loss landscapes for the STU, S4, and attention layers, respectively, after 10 steps of training on the LDS. Figures 15- 17 in Appendix B instead visualize the local geometry through sharpness in terms of Hessian eigenvalue ratios. Flatter minima are preferable since it has been proposed that reducing sharpness helps with generalization [10]. One of the main strengths of the STU is its clean and saddle-free optimization landscape; this benefit becomes more important in larger and more complex models.

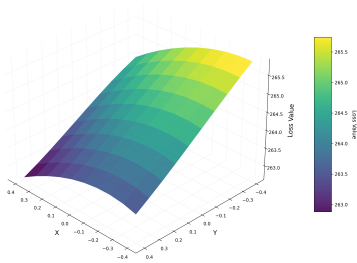


Figure 3: Local loss landscape of the STU layer

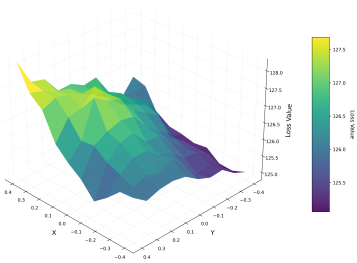


Figure 4: Local loss landscape of the S4 layer

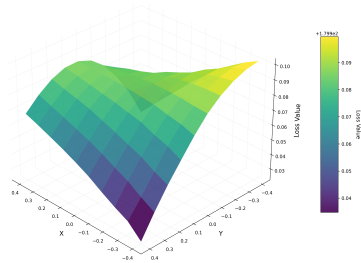


Figure 5: Local loss landscape of the attention layer

2.3 Other synthetic tasks

We also investigate the performance of the STU layer in synthetic tasks that are more well-known in the deep learning literature. We briefly introduce the induction heads [13] and associative recall [11] tasks, our experimental setups, and the corresponding results here. For completeness, we include in Appendix B the results on other tasks including selective copy [3] and a novel **mode prediction task** that may be independently useful.

In the induction heads task, the model is required to memorize one token (sampled uniformly from a vocabulary) immediately after a special `flag` token; the rest of the context consists of the same special `blank` token, which the model should learn to ignore. The associative recall task is slightly different, as it first gives the model an (unordered) sequence of key-value pairs and then asks for the value associated with a query key after – the model must memorize the entire context, not just a single token. Both of these tasks have nonlinear dynamics and require single-token precision to fully solve; furthermore, since we apply deeper models, the optimizations are nonconvex for all the models considered.

Experiment details and conclusions. We trained two-layer models (with MLP layers in between) using the cross-entropy loss, the Adam optimizer with default PyTorch parameters, and batches of size 32. We set the context length to 32 and all the model widths to 32. In addition, the attention model has 8 heads and the S4 model has hidden dimension 64. For induction heads, the vocabulary size is 4. We plot the accuracies during training for induction heads and selective copy in Figures 6 and 7, respectively, averaged over 8 trials with error bars.

As we can see, on both tasks the STU is able to solve the task quickly and consistently. By contrast, on the induction heads task we see that STU-T and the attention and S4 baselines appear to learn in stages, with the accuracy plateauing occasionally. Furthermore, there is significant variation across seeds for which timestep the attention model begins to solve the task. Both of these observations point to the difficulty of the underlying optimization problem: while all models considered are expressive enough to solve induction heads, the STU appears to have an easier time finding such a solution.

On the associative recall task, we see a similar story. The SSM models all converge very quickly, while the attention-based model requires more optimization steps and learns more gradually. These results are particularly surprising considering that the tasks involved feel difficult to approximate by linear dynamics, so one might have expected the nonlinear, non-dynamical structure of softmax attention to dominate here.

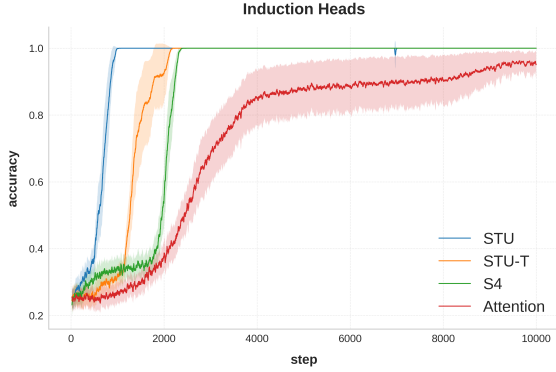


Figure 6: Prediction accuracy for the token immediately following the special flag token during training

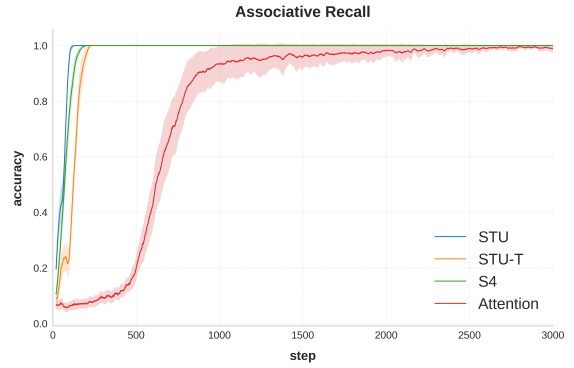


Figure 7: Prediction accuracy for the value corresponding to the given query during training

Overall, the optimization behavior of STU on these synthetic tasks give us confidence that it is a simple, easily optimizable, yet expressive layer for use in larger models, which will be the main focus for the rest of the paper.

3 Experiments with robotics sequence prediction

We now consider next-state prediction using the MuJoCo physics engine [32], a more challenging sequence prediction task. The goal is to learn the dynamics of a certain physical simulation agent, for example the `Ant-v1` system,

$$x_{t+1} = f(x_t, u_t), \quad (1)$$

where $x_t \in \mathbb{R}^{29}$ and $u_t \in \mathbb{R}^8$ correspond to the state and action at time t , respectively.

More precisely, x_t corresponds to the positions, orientations, joint angles, and velocities of the various limbs of the `Ant-v1` controller, whereas u_t represents the torques applied to the joints of the `Ant-v1` controller and are generated from a pretrained proximal policy optimization [28]. Unlike the synthetic linear dynamical system in Section 2, the dynamics f for this particular MuJoCo prediction task are nonlinear and hybrid, i.e. non-smooth.

In the experiments below, we defined the loss function to be the squared Euclidean distance between the predicted state vector \hat{x}_{t+1} and the true state vector x_{t+1}

$$L(\theta) = \frac{1}{2} \|\hat{x}_{t+1}(\theta) - x_{t+1}\|_2^2 = \frac{1}{2} \sum_{i=1}^n (\hat{x}_{t+1,i}(\theta) - x_{t+1,i})^2,$$

where $\hat{x}_{t+1}(\theta)$ is the predicted state vector parameterized by θ , and x_{t+1} is the true state vector.

Model architectures. The Mixture-of-Experts (MoE) architecture has seen newfound resurgence in modern neural networks thanks to its ability to increase model capacity without a proportional increase in computation [30]. We ran small ablation studies and found that a sparsely mixture-of-experts (MoE) over gated MLPs after the model’s main sublayer performed the best. The gated MLP splits the inputs into two parts: a main component and a "gate" that modulates the main component using the SiLU [27] activation function. The gating MoE network then dynamically selects which top experts to use for each input based on a learned distribution, where each expert is a gated MLP, applies the `top_k` selected expert(s) to the input, and combines their outputs using a weighted summation, where the weights come from the gating mechanism. Figure 20 shows the model architectures in detail. Table 1 gives the specification for

each tested architecture in these two sets of experiments.

We attempted to maintain the same parameter count 0.5M for each model given the various architectural differences which are presented in Section A of the appendix. For STU, Transformer, and Mamba-2 models, we ensured that they have the same widths and depths and, following [34], only adjusted the MLP expansion factor as the primary method to equalize the parameter count. As for the STU-T model, its tensor dot approximation allowed for extra parameter space that can be allocated towards other areas in the model. For example, using exactly the same configurations as STU, STU-T only has 0.05M parameters; to scale it up for fair model comparisons, here we choose to expand the "width" of STU-T, which is the model dimension d_{model} in Figure 1.

Experiment controllers. We tested our models on three MuJoCo controllers: `Ant-v1`, `HalfCheetah-v1`, and `Walker2D-v1`. The full results are in Section B of the appendix; we only provide results for `Ant-v1` here for illustration (Figure 8 and Table 2). We also note that the results presented hereby are partial, after hyperparameter tuning. The full results of these ablation studies can be found in Section D.1.

Additional experiments. To further validate the results, we conduct next-step prediction and autoregressive next-step prediction using the trained models (Figure 9 and 10). Next-step prediction uses ground-truth states and actions from a fixed input window to forecast the next state, mirroring the model’s training evaluation. Autoregressive next-step prediction, however, incorporates the model’s own past predictions as inputs, illustrating how errors accumulate over time.

Table 1: Model Specifications for the `Ant-v1` Task

Model	Parameters	Width/Depth	MLP Scale	Filters	MoE	Time/Step
STU	0.55M	64/4	1	16^4	False	11.4ms
STU-T	0.47M	128/4	8	16	False	11.4ms
Transformer	0.51M	64/4	6	-	True	21.3ms
Mamba-2	0.51M	64/4	4	-	True	40.5ms

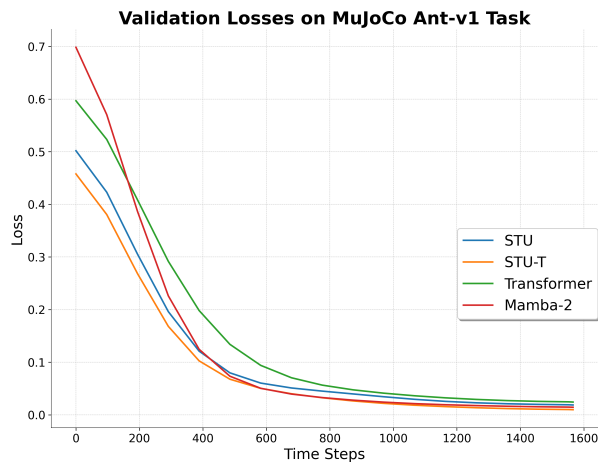


Figure 8: `Ant-v1` comparative training results

Table 2: `Ant-v1` comparative validation loss results

Model	Validation Loss
STU	0.0181
STU-T	0.0092
Transformer	0.0237
Mamba-2	0.0139

⁴Ablation studies on the performance of STU using different number of filters (K) show that at around $K = 15$ loss stops decaying exponentially and plateaus[1].

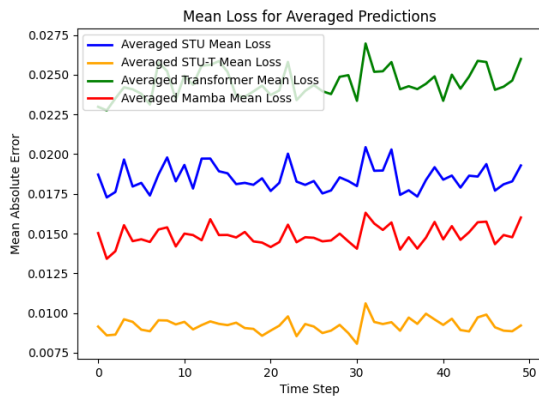


Figure 9: Ant-v1 comparative next-step prediction results (with losses averaged over 500 predictions for each model)

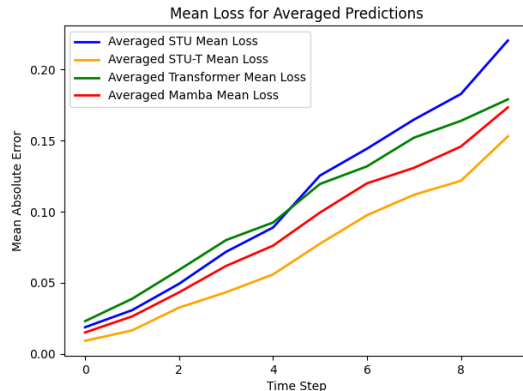


Figure 10: Ant-v1 comparative autoregressive next-step prediction results (with losses averaged over 500 predictions for each model)

3.1 Takeaways from robotics experiments

As can be seen in the experiment results, on a parameter-adjusted basis, the STU-T outperforms all other models.

Attention vs. State Space Models. It has been observed that Transformers struggle with tasks requiring the recall of long-range dependencies [31], whereas state space models (SSMs) excel in this aspect. Transformers’ quadratic complexity in sequence length [33] contrasts with SSMs’ linear complexity and ability to theoretically capture infinitely long dependencies [14]. Mamba [13], a recent SSM variant, introduces selective state spaces that dynamically adapt to input sequences, achieving state-of-the-art performance across various tasks. In our study, Mamba-2 indeed significantly outperforms Transformer in MuJoCo robotics sequence prediction tasks. More excitingly, our STU-T performs even better than Mamba-2 (and faster), demonstrating its potential in pushing the boundaries of performance and efficiency.

Tensor dot approximation effect. As noted in the introduction, the tensor dot approximation of STU-T models is a significant optimization in both computational and memory efficiency. We found that STU-T models are much smaller yet have performance on par, and at most times exceeding, that of full STU models. Moreover, the parameter savings due to the tensor dot approximation can be reallocated towards other areas of the model. This makes STU-T models our best performing variant given equalized parameter counts, beating state-of-the-art Mamba-2 model in all three MuJoCo tasks.

Mixture-of-STUs. We found that formulating our MLP layer in the SwiGLU configuration [29] improves performance in STU models; however, formulating the MLP layer as a sparsely-gated mixture-of-SwiGLUs hurts performance. We envision there is a ripe field of research in architectural design for the STU waiting to be explored, e.g. adaptive online methods and variants of MoE [15], which we leave to future work.

Width vs. Depth. The STU model benefits more from increasing model depth, whereas the Transformer model is more sensitive to increases in model width. When model width is held constant, we observe that the Transformer’s performance gains stagnate early with respect to depth—particularly after just two layers. We suspect this is related to the ‘induction heads’ phenomenon observed in attention-based architectures [23]. Induction heads are specialized attention mechanisms that enable the model to recognize and replicate patterns in the input data, facilitating in-context learning. These heads typically emerge within the first two layers of a Transformer, providing the bulk of its learning capabilities. As a result, additional layers contribute diminishing returns, since the core functionalities are already established early on. Despite the apparent absence of induction head circuits in the STU, it still performs well on the MuJoCo task, outperforming the Transformer.

Noise. We introduced zero-mean Gaussian noise with standard deviation defined by the `noise` parameter applied with probability p at each time step. From Table 7, 8, and 9, we can see that the STU is more resistant to such noise compared to the Transformer, suggesting that the STU could be less prone to overfitting.

4 Experiments with language modeling

In this section, we explore the STU’s ability for sequence prediction in the context of language modeling. We model our architecture in the style of GPT-2 [26], and we open source a simple, fully distributed large language model (LLM) pretraining pipeline [22] for the community to enjoy and build upon.

4.1 Experiment setup

Data. We pretrain on roughly 10B high-quality tokens from FineWeb-Edu [24], a large-scale, open source dataset for language modeling. We tokenized the dataset into 95 training shards and 1 validation shard, each containing about 100M tokens, using the `o200k_base` tokenizer from the OpenAI `tiktoken`⁵ library.

General design choices. For each model, we used RMSNorm [36] to pre-normalize the inputs before each attention layer, Flash STU layer, and MLP layer. We followed the standard pre-norm residual connection pattern around each of the sublayers, i.e. the output of each sublayer is $x + \text{Sublayer}(\text{RMSNorm}(x))$. To further stabilize training, we capped logits [4, 35] in each attention layer at 50.0. Following NanoGPT, we rounded up the vocabulary size of each model to the nearest multiple of 64 in order to use more efficient CUDA kernel pathways. We tied embeddings, and we did not use dropout.

Transformer architecture. We followed the GPT-2-styled Transformer from NanoGPT [19]. We added small optimizations such as FlashAttention-2 [7] and the ALiBi [25] modification to the attention scores. We used position interpolation [6] to help the model "length generalize" beyond its context window size from training. It has been shown that position interpolation works even with ALiBi [2], so we used an interpolation factor of 0.25, extending the model’s effective context window size at inference time by a factor of 4. We used highly optimized Triton⁶ kernels [18] for the implementation of our MLP (SwiGLU), RMSNorm, and loss function.

Flash STU architecture. We augmented the STU-T model with Flash FFT [12] for efficient convolutions. We found that the `tensor_dot` approximation was necessary to scale up STU-based models, as it was difficult to scale beyond 1B parameters without experiencing frequent out-of-memory (OOM) errors. Following the work from the state space literature [8, 34] relating to the role of attention layers, we opted to use a simple *hybrid* model architecture with alternating layers consisting of STU-T and local attention, both followed by an MLP layer. We used the same optimized Triton kernels from the Transformer, and we replaced global attention with sliding window attention [5].

⁵<https://github.com/openai/tiktoken/>

⁶<https://openai.com/index/triton/>

Flash STU Model Architecture

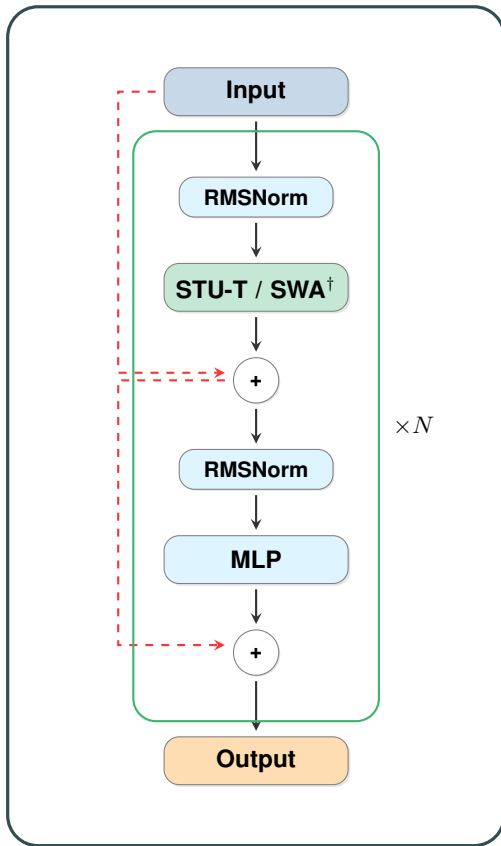


Figure 11: Flash STU Model Architecture, alternating between STU-T and (sliding window) attention[†]

Training. We used fused AdamW [21] with default PyTorch hyperparameters, and we set the maximum learning rate and minimum learning rate to 3.0×10^{-4} and 3.0×10^{-5} , respectively. We followed a linear decay with warmup learning rate schedule [9] and allocated 10% of the total number of training steps towards warming up the learning rate to the maximum learning rate, per [17], before linearly decaying back down to the minimum learning for the remainder of the training run. For better memory efficiency, we accumulated gradients and performed gradient updates only after every 8 training steps. Each model was trained for 16 hours across $8 \times \text{H100}$ 80GB HBM3 GPUs using the Fully Sharded Data Parallel (FSDP) framework from PyTorch [37].

4.2 Results

Table 3 summarizes the key performance metrics for both models. We found that the Flash STU model outperformed the Transformer model in terms of validation loss and perplexity. Sample autoregressive text generation from the Flash STU model can be found in Appendix E. For completeness, we included the performances of the two variants of STU-T as well in Figure 27.

Table 3: Performance Comparison of Flash STU and Transformer Models

Model	Validation Loss	Perplexity	Mean Time/Step
Flash STU	3.09	22.08	≈ 3.0s
Transformer	3.18	24.11	

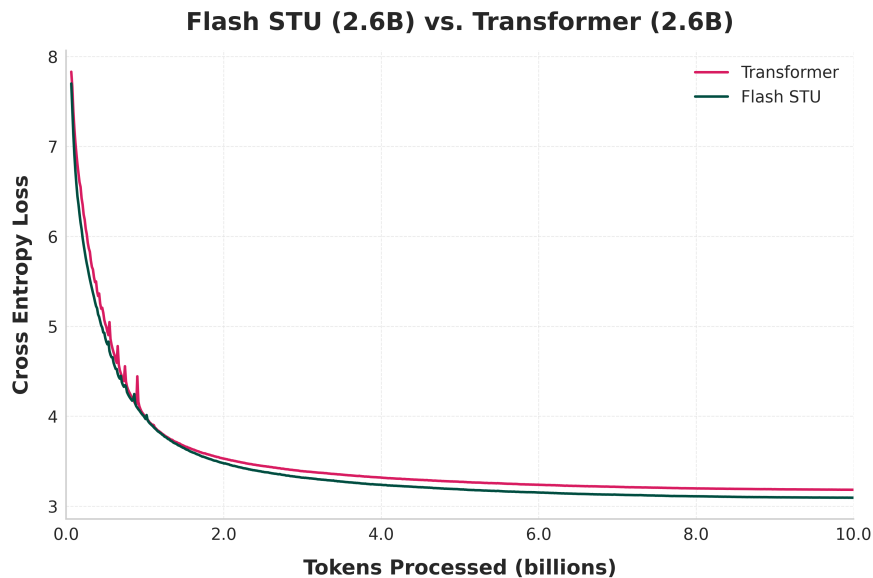


Figure 12: Comparison of Flash STU and Transformer models on validation set

Qualitatively, we found that the Transformer was more sensitive to hyperparameter tuning, e.g. learning rate. Additionally, the Transformer was more prone to spikes in its loss compared to Flash STU despite our best attempts to stabilize training.

We also note that although our Flash STU implementation is fairly optimized, it is not yet at the level at which the community has optimized the Transformer model in recent years. Although Flash STU has the edge in terms of asymptotic time complexity, the Transformer is heavily optimized for matrix multiplication units on modern accelerator hardware, which generally translates to superior wall-clock performance in practice. However, we notably found that the average time per step was approximately around the same for both models. Thus, we believe that the Flash STU model demonstrates great promise for future improvements given that it outperformed the Transformer while having an asymptotically better time complexity.

4.3 Finetuning filters

The core building block of the spectral state space model is the spectral filter, described in more detail in Appendix A. Slightly deviating from the originally proposed Spectral State Space model architecture, we ran an ablation training run where we initialized the K filters from the Hankel matrix per usual following the theory of spectral filtering but made the filters at each layer to be learnable parameters with a learning rate equivalent to that of the main model architecture.

Interestingly enough, this slightly improved the performance of Flash STU, but we do not yet make any strong claims about this observation and leave this to future work under a more rigorous experimentation framework.

Table 4: Performance Comparison of Flash STU and Transformer Models

Model	Validation Loss	Perplexity	Mean Time/Step
Flash STU	3.00	20.11	≈ 3.0s
Transformer	3.18	24.11	

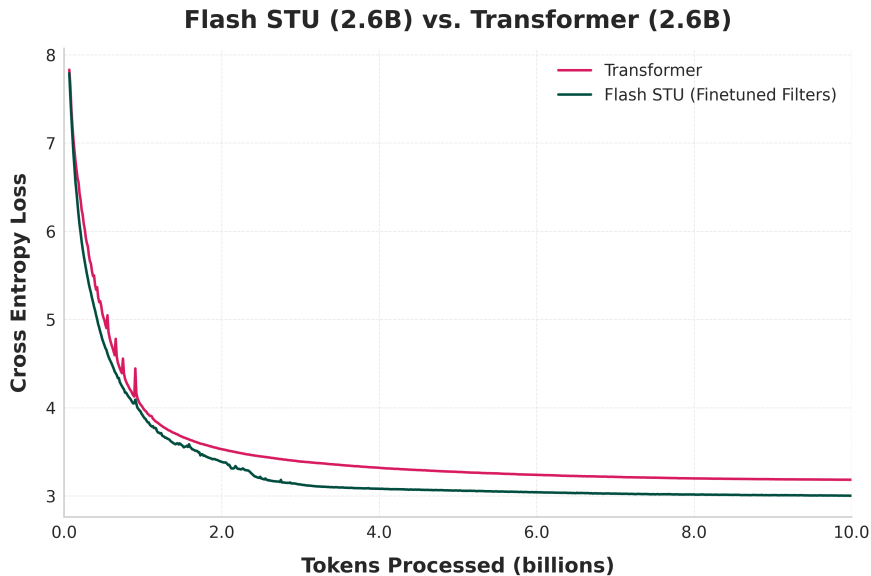


Figure 13: Finetuning the Flash STU spectral filters improves its performance vs. Transformer over 10B tokens

5 Conclusions and future directions

This paper presented an experimental overview of the new theoretically-founded deep neural architecture of spectral transformers [1] on three different modalities: synthetic data, robotics control sequences, and language modeling. We find that the STU is a viable alternative relative to other popular sequence models, notably the Transformer and various other state space models. Our experiments were coupled with highly optimized open source software available at [22].

The theoretical guarantees of the STU, notably its ability to handle large context efficiently, is yet to be investigated thoroughly, which we leave for future work.

6 Acknowledgements

Windsor Nguyen, Isabel Liu, Yagiz Devre and Evan Dogariu were funded in part by Elad Hazan’s grants from the Office of Naval Research and the National Science Foundation. We would like to give special thanks to Princeton Research Computing⁷ and Princeton Language and Intelligence⁸ (PLI) for supplying us with the compute required for making our experiments possible.

⁷<https://researchcomputing.princeton.edu/>

⁸<https://pli.princeton.edu/>

References

- [1] Naman Agarwal, Daniel Suo, Xinyi Chen, and Elad Hazan. Spectral State Space Models. *arXiv preprint arXiv:2312.06837*, 2023.
- [2] Faisal Al-Khateeb, Nolan Dey, Daria Soboleva, and Joel Hestness. Position Interpolation Improves ALiBi Extrapolation, 2023.
- [3] Martin Arjovsky, Amar Shah, and Yoshua Bengio. Unitary Evolution Recurrent Neural Networks. In *Proceedings of The 33rd International Conference on Machine Learning*, pages 1120–1128, 2016.
- [4] Irwan Bello, Hieu Pham, Quoc V. Le, Mohammad Norouzi, and Samy Bengio. Neural Combinatorial Optimization with Reinforcement Learning, 2017.
- [5] Iz Beltagy, Matthew E. Peters, and Arman Cohan. Longformer: The Long-Document Transformer, 2020.
- [6] Shouyuan Chen, Sherman Wong, Liangjian Chen, and Yuandong Tian. Extending Context Window of Large Language Models via Positional Interpolation, 2023.
- [7] Tri Dao, Daniel Y. Fu, Stefano Ermon, Atri Rudra, and Christopher Ré. FlashAttention: Fast and Memory-Efficient Exact Attention with IO-Awareness, 2022.
- [8] Tri Dao and Albert Gu. Transformers are SSMS: Generalized Models and Efficient Algorithms Through Structured State Space Duality, 2024.
- [9] Aaron Defazio, Ashok Cutkosky, Harsh Mehta, and Konstantin Mishchenko. When, Why and How Much? Adaptive Learning Rate Scheduling by Refinement, 2023.
- [10] Pierre Foret, Ariel Kleiner, Hossein Mobahi, and Behnam Neyshabur. Sharpness-Aware Minimization for Efficiently Improving Generalization, 2020.
- [11] Daniel Y. Fu, Tri Dao, Khaled K. Saab, Armin W. Thomas, Atri Rudra, and Christopher Ré. Hungry Hungry Hippos: Towards Language Modeling with State Space Models, 2023.
- [12] Daniel Y. Fu, Hermann Kumbong, Eric Nguyen, and Christopher Ré. FlashFFTConv: Efficient Convolutions for Long Sequences with Tensor Cores, 2023.
- [13] Albert Gu and Tri Dao. Mamba: Linear-Time Sequence Modeling with Selective State Spaces, 2024.
- [14] Albert Gu, Karan Goel, and Christopher Ré. Efficiently Modeling Long Sequences with Structured State Spaces, 2022.
- [15] Elad Hazan and Karan Singh. Introduction to Online Nonstochastic Control. *arXiv preprint arXiv:2211.09619*, 2022.
- [16] Elad Hazan, Karan Singh, and Cyril Zhang. Learning Linear Dynamical Systems via Spectral Filtering. *Advances in Neural Information Processing Systems*, 30, 2017.
- [17] Jordan Hoffmann, Sebastian Borgeaud, Arthur Mensch, Elena Buchatskaya, Trevor Cai, Eliza Rutherford, Diego de Las Casas, Lisa Anne Hendricks, Johannes Welbl, Aidan Clark, Tom Hennigan, Eric Noland, Katie Millican, George van den Driessche, Bogdan Damoc, Aurelia Guy, Simon Osindero, Karen Simonyan, Erich Elsen, Jack W. Rae, Oriol Vinyals, and Laurent Sifre. Training Compute-Optimal Large Language Models, 2022.
- [18] Byron Hsu. Liger-Kernel. <https://github.com/linkedin/Liger-Kernel>, 2024.
- [19] Andrej Karpathy. build-nanogpt. <https://github.com/karpathy/build-nanogpt>, 2024.
- [20] Hao Li, Zheng Xu, Gavin Taylor, Christoph Studer, and Tom Goldstein. Visualizing the Loss Landscape of Neural Nets, 2017.

- [21] Ilya Loshchilov and Frank Hutter. Decoupled Weight Decay Regularization, 2019.
- [22] Windsor Nguyen and contributors. Flash STU Repository. <https://github.com/windsornguyen/flash-stu>, 2024.
- [23] Catherine Olsson, Nelson Elhage, Neel Nanda, Nicholas Joseph, Nova DasSarma, Tom Henighan, Ben Mann, Amanda Askell, Yuntao Bai, Anna Chen, Tom Conerly, Dawn Drain, Deep Ganguli, Zac Hatfield-Dodds, Danny Hernandez, Scott Johnston, Andy Jones, Jackson Kernion, Liane Lovitt, Kamal Ndousse, Dario Amodei, Tom Brown, Jack Clark, Jared Kaplan, Sam McCandlish, and Chris Olah. In-context Learning and Induction Heads, 2022.
- [24] Guilherme Penedo, Hynek Kydlíček, Loubna Ben allal, Anton Lozhkov, Margaret Mitchell, Colin Raffel, Leandro Von Werra, and Thomas Wolf. The FineWeb Datasets: Decanting the Web for the Finest Text Data at Scale, 2024.
- [25] Ofir Press, Noah A. Smith, and Mike Lewis. Train Short, Test Long: Attention with Linear Biases Enables Input Length Extrapolation, 2022.
- [26] Alec Radford, Jeffrey Wu, Rewon Child, David Luan, Dario Amodei, Ilya Sutskever, et al. Language models are unsupervised multitask learners. *OpenAI Blog*, 1(8):9, 2019.
- [27] Prajit Ramachandran, Barret Zoph, and Quoc V. Le. Searching for Activation Functions, 2017.
- [28] John Schulman, Filip Wolski, Prafulla Dhariwal, Alec Radford, and Oleg Klimov. Proximal Policy Optimization Algorithms, 2017.
- [29] Noam Shazeer. GLU Variants Improve Transformer, 2020.
- [30] Noam Shazeer, Azalia Mirhoseini, Krzysztof Maziarz, Andy Davis, Quoc Le, Geoffrey Hinton, and Jeff Dean. Outrageously Large Neural Networks: The Sparsely-Gated Mixture-of-Experts Layer, 2017.
- [31] Yi Tay, Mostafa Dehghani, Samira Abnar, Yikang Shen, Dara Bahri, Philip Pham, Jinfeng Rao, Liu Yang, Sebastian Ruder, and Donald Metzler. Long Range Arena: A Benchmark for Efficient Transformers, 2020.
- [32] Emanuel Todorov, Tom Erez, and Yuval Tassa. MuJoCo: A physics engine for model-based control. In *2012 IEEE/RSJ International Conference on Intelligent Robots and Systems*, pages 5026–5033. IEEE, 2012.
- [33] Ashish Vaswani, Noam Shazeer, Niki Parmar, Jakob Uszkoreit, Llion Jones, Aidan N. Gomez, Lukasz Kaiser, and Illia Polosukhin. Attention Is All You Need, 2017.
- [34] Roger Waleffe, Wonmin Byeon, Duncan Riach, Brandon Norick, Vijay Korthikanti, Tri Dao, Albert Gu, Ali Hatamizadeh, Sudhakar Singh, Deepak Narayanan, Garvit Kulshreshtha, Vartika Singh, Jared Casper, Jan Kautz, Mohammad Shoeybi, and Bryan Catanzaro. An Empirical Study of Mamba-based Language Models, 2024.
- [35] xAI. Grok 1 open release. <https://github.com/xai-org/grok-1>, 2024.
- [36] Biao Zhang and Rico Sennrich. Root Mean Square Layer Normalization, 2019.
- [37] Yanli Zhao, Andrew Gu, Rohan Varma, Liang Luo, Chien-Chin Huang, Min Xu, Less Wright, Hamid Shojanazeri, Myle Ott, Sam Shleifer, Alban Desmaison, Can Balioglu, Pritam Damania, Bernard Nguyen, Geeta Chauhan, Yuchen Hao, Ajit Mathews, and Shen Li. PyTorch FSDP: Experiences on Scaling Fully Sharded Data Parallel, 2023.

A Spectral filters

Following [1], we construct spectral filters by extracting the top K eigenvectors from the Hankel matrix:

$$Z = \frac{2}{(i+j)^3 - (i+j)}, \quad (2)$$

or, alternatively, from

$$Z_L = ((-1)^{i+j-2} + 1) \cdot \frac{8}{(i+j+3)(i+j-1)(i+j+1)} \quad (3)$$

These top K eigenvectors are then scaled by their corresponding eigenvalues, each raised to the $\frac{1}{4}$ -th power. These scaled eigenvectors serve as our spectral filters and are used to convolve inputs into the spectral basis.

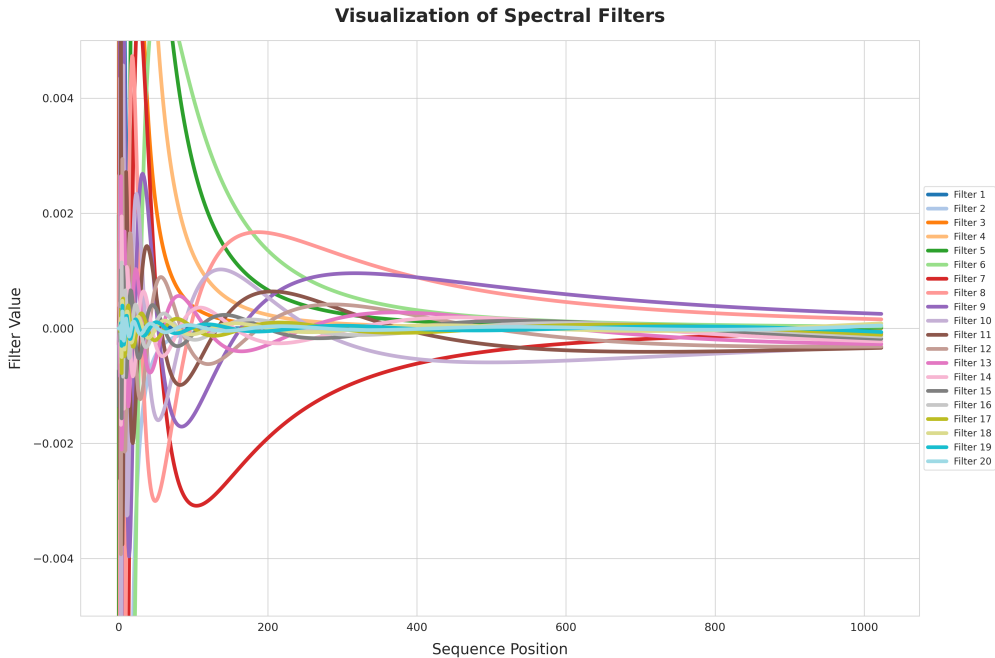


Figure 14: Visualization of the first 20 spectral filters used in our STU-based models

B Additional synthetic experiments

Extra experimental details. The synthetic experiments were all run on a single A100 GPU, with each trial for each model taking around a minute to complete. The STU implementation followed Figure 1 exactly, with the tensor dot approximation replacing the STU layer in the STU-T implementation. The softmax attention baseline is FlashAttention [7], and for S4 we used the official implementation [14]. Wherever we introduce nonlinearities in the synthetic experiments it is always ReLU; we leave a close investigation of multiplicative gating nonlinearities like GLU to future work.

Local sharpness of the loss. In Figures 15-17, the sharpness values of the loss Hessian are plotted after 10 steps of training on the LDS task from the main paper. A ratio near 1.0 means the curvature is similar in all directions, while a ratio near 0.0 means the curvature is stronger in one direction. We use absolute value because we are interested in the

magnitude of the curvature. The contour lines overlaid on the heatmap show the loss landscape, allowing us to visualize how local convexity relates to the overall loss surface. Blue areas represent more spherical curvature, and red areas represent more elongated curvature. Movement along the x and y axes corresponds to local movement in parameter space.

For STU, we see very smooth behavior and an obvious direction of progress toward well-conditioned areas, whereas the loss landscape is more complicated for S4 and attention.

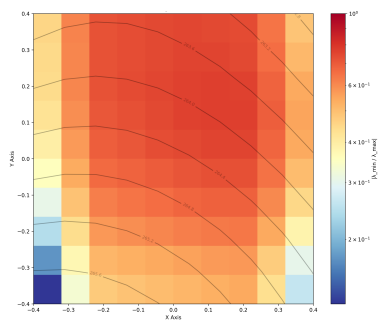


Figure 15: Heatmap of the ratio $|\lambda_{\min}/\lambda_{\max}|$ of (an estimate of a dimensionality-reduced version of) the loss Hessian for an **STU** layer

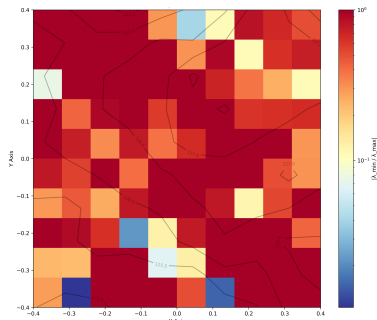


Figure 16: Heatmap of the ratio $|\lambda_{\min}/\lambda_{\max}|$ of (an estimate of a dimensionality-reduced version of) the loss Hessian for an **S4** layer

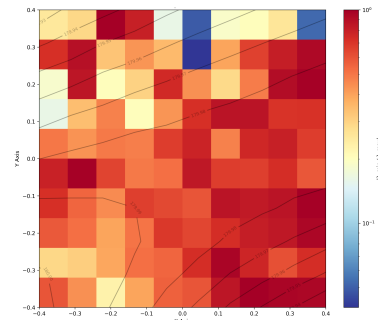


Figure 17: Heatmap of the ratio $|\lambda_{\min}/\lambda_{\max}|$ of (an estimate of a dimensionality-reduced version of) the loss Hessian for an **attention** layer

Other tasks. For a comprehensive study of how the STU layer performs on different types of small sequence prediction problems, we also experiment on the selective copy task [3] and prediction of the mode of the tokens in the context⁹. The selective copy task requires the model to recall (in order) a sequence of a fixed number of tokens (which are sampled uniformly from a vocabulary and distributed randomly throughout the context of otherwise `blank` tokens). By contrast, the mode prediction task simply requires the model to output the mode of a sequence of tokens sampled randomly from a vocabulary.

Speaking broadly, an LDS requires a structured aggregation of the context, while induction heads requires only local understanding of the context. Mode prediction and selective copy combine these principles, testing a model’s ability to synthesize single-token-precision information across the whole sequence. Training results are presented in Figures 18 and 19, respectively.

⁹As far as we can tell, a task involving prediction of the mode of discrete data has not been used to study the behaviors of sequence models in any existing literature. We think it is an elegant way to probe a model’s ability to nonlinearly synthesize very simple single-token information, as it is clear how the difficulty of the problem scales with sequence length and vocabulary size. It may also lend itself to strong theoretical analyses on account of its simplicity, and there is clear structure with which to study generalization to new tokens or sequence lengths.

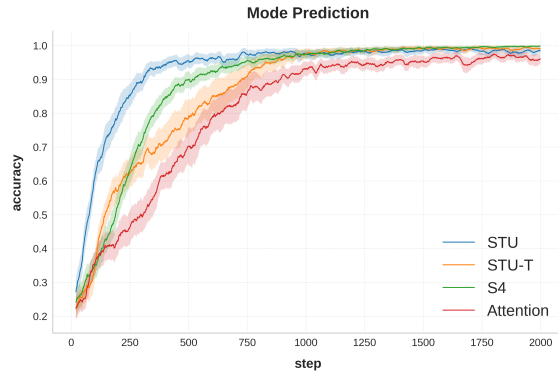


Figure 18: Prediction accuracy for the mode of the context during training

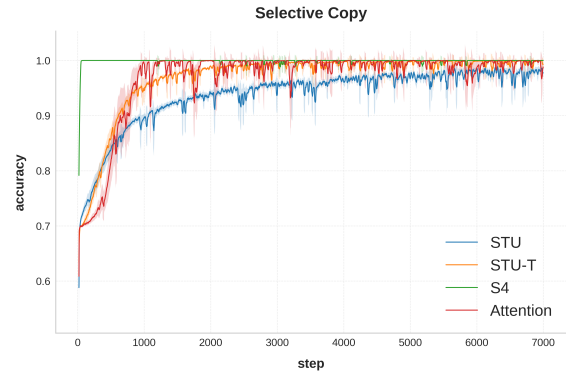


Figure 19: Prediction accuracy for repeating the non-blank tokens in the context during training

Experiment details and conclusions. As before, we train two-layer models with MLP layers with nonlinearities in between. The models are trained for the number of steps shown with the Adam optimizer with default parameters. Both tasks are constructed with a sequence length of 32, and for mode prediction we use a small vocabulary of 5 tokens.

On mode prediction, we see the same surprising results as on induction heads and associative recall: SSM models perform learn the quickest, with STU leading the way. However, the S4 model dominates on selective copy, while STU-T appears able to match the attention baseline. All models eventually converge to perfect accuracy and are always able to express a solution for this task, but this time it is S4 that appears to have the easiest optimization. *{evan: does this result make sense? its the only place STU doesnt win}*

To see empirical results between STU and S4 on the Long Range Arena benchmark, see Table 1 of [1].

C Additional model architectures

Figure 20 shows the model architectures used for the robotics experiments in section 3. We ran small ablation studies and found that global skip connections oftentimes improved performance in our MuJoCo robotics experiment setting. In non-hybrid STU architectures, we found that performance decreases when using an MoE architecture, as discussed in 3.1, so we used a simple gated MLP instead.

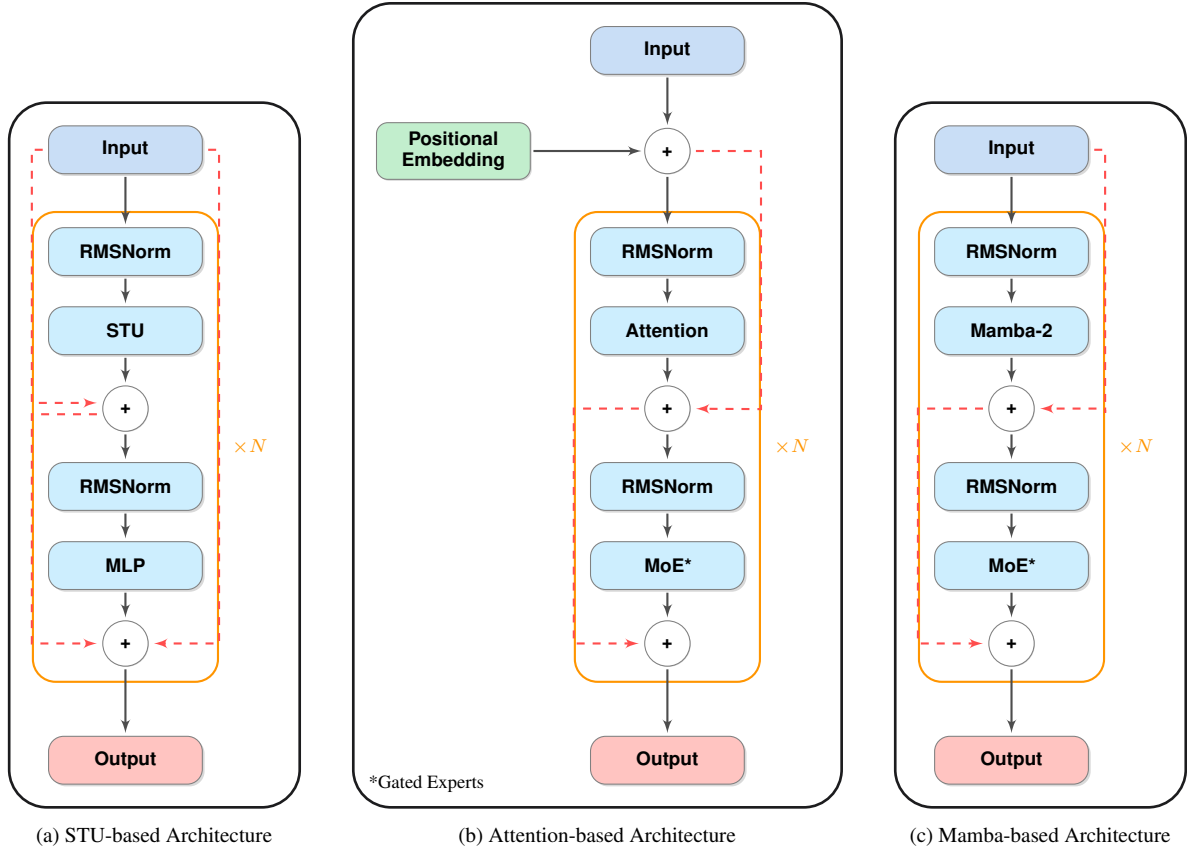


Figure 20: Comparison of STU-based, Attention-based, and Mamba-based model architectures

D Additional experiments with robotics data

In this section we give the remaining experimental results over robotics data for the other two MuJoCo tasks: HalfCheetah-v1 and Walker2D-v1. Compared to Ant-v1 (shown in Section 2 in the main paper), these two tasks only involve motion in a 2D plane. As a result, the state representations for HalfCheetah-v1 and Walker2D-v1 are inherently less complex, potentially affecting the relative performance of different models on these tasks in theory.

In this setting, the comparison of the models' performances still remains consistent, with Transformer showing the least competitive results, Mamba-2 demonstrating significant improvements over Transformer, and STU-T outperforming both Transformer and Mamba-2. HalfCheetah-v1 task's training results are shown in Figure 21 and Table 5, (auto-regressive) next-step predictions results in Figure 22 and Figure 23. Walker2D-v1 task's training results are shown in Figure 24 and Table 6, (auto-regressive) next-step predictions results in Figure 25 and Figure 26.

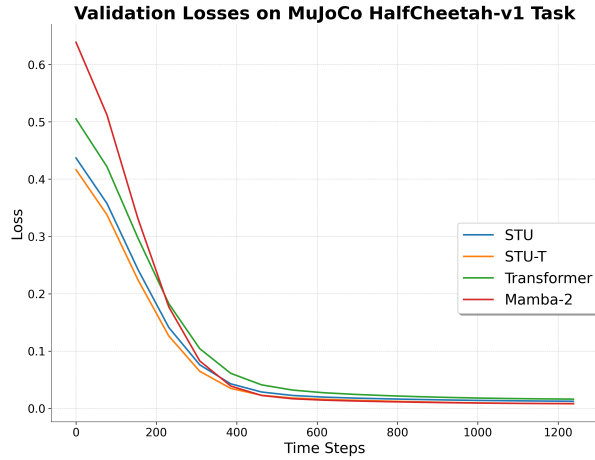


Figure 21: HalfCheetah-v1 comparative training results

Table 5: HalfCheetah-v1 comparative validation loss results

Model	Validation Loss
STU	0.0119
STU-T	0.0076
Transformer	0.0157
Mamba-2	0.0081

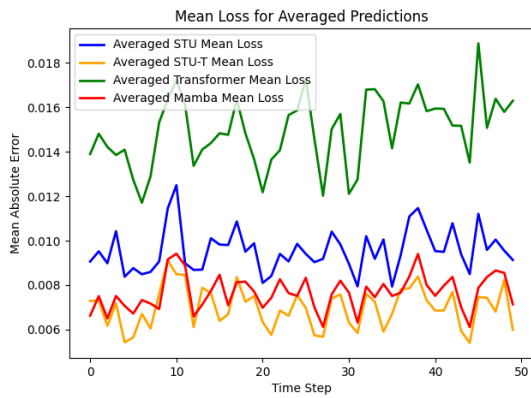


Figure 22: HalfCheetah-v1 comparative next-step prediction results (with losses averaged over 500 predictions for each model)

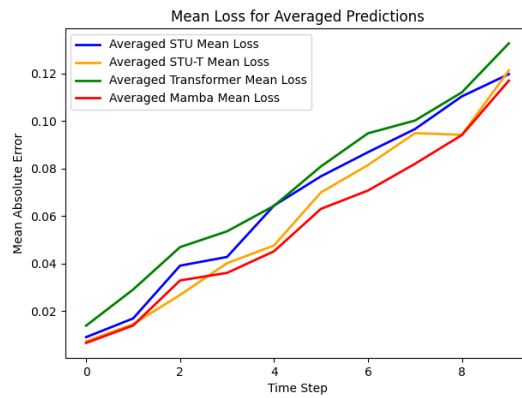


Figure 23: HalfCheetah-v1 comparative auto-regressive next-step prediction results (with losses averaged over 500 predictions for each model)

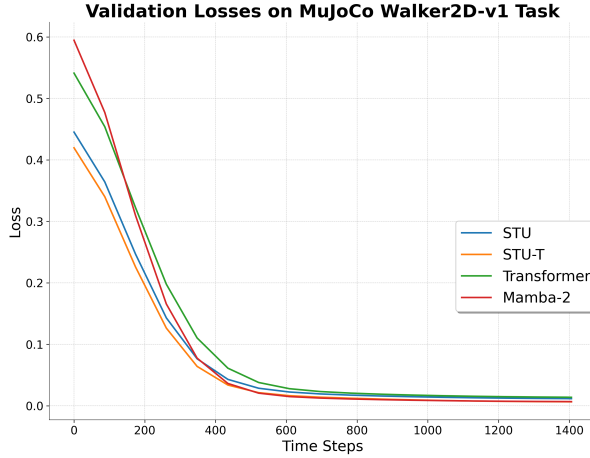


Figure 24: Walker2D-v1 comparative training results

Table 6: Walker2D-v1 comparative validation loss results

Model	Validation Loss
STU	0.0112
STU-T	0.0062
Transformer	0.0134
Mamba-2	0.0066

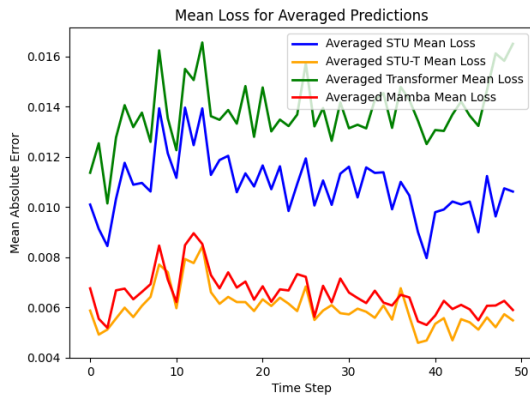


Figure 25: Walker2D-v1 comparative next-step prediction results (with losses averaged over 500 predictions for each model)

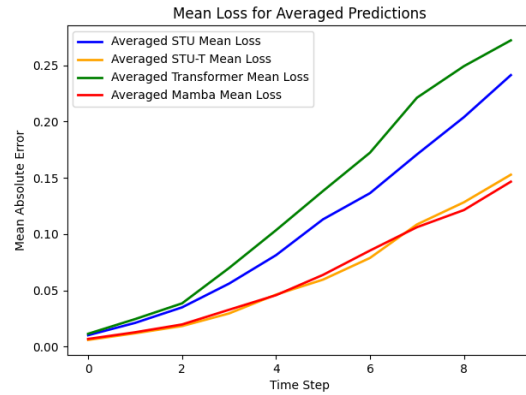


Figure 26: Walker2D-v1 comparative auto-regressive next-step prediction results (with losses averaged over 500 predictions for each model)

D.1 Hyperparameters for robotics experiments

We conducted comprehensive ablation studies to investigate the impact of various hyperparameters on the performance of STU, STU-T, and Transformer models in the context of robotics tasks. These studies explore the effects of model width, depth, and input noise on the final Mean Squared Error (MSE) loss. Tables 7, 8, and 9 present the results of these experiments.

Table 7: Ablation studies for STU Models

Model	Parameter Count	Width	Layers	Noise/Frequency	MSE Loss
STU	0.18M	32	4	0.0/0.0	0.0217
STU	0.63M	64	4	0.0/0.0	0.0139
STU	1.33M	96	4	0.0/0.0	0.0120
STU	2.30M	128	4	0.0/0.0	0.0108
STU	0.05M	32	1	0.0/0.0	0.0449
STU	0.09M	32	2	0.0/0.0	0.0306
STU	0.18M	32	4	0.0/0.0	0.0217
STU	0.27M	32	6	0.0/0.0	0.0203
STU	0.18M	32	4	0.0/0.0	0.0217
STU	0.18M	32	4	0.1/0.1	0.0357
STU	0.18M	32	4	0.5/0.1	0.0561

Table 8: Ablation studies for STU-T Models

STU-T	0.06M	32	4	0.0/0.0	0.0239
STU-T	0.12M	64	4	0.0/0.0	0.0146
STU-T	0.20M	96	4	0.0/0.0	0.0116
STU-T	0.28M	128	4	0.0/0.0	0.0105
STU-T	0.02M	32	1	0.0/0.0	0.0464
STU-T	0.03M	32	2	0.0/0.0	0.0328
STU-T	0.06M	32	4	0.0/0.0	0.0239
STU-T	0.09M	32	6	0.0/0.0	0.0218
STU-T	0.06M	32	4	0.0/0.0	0.0239
STU-T	0.06M	32	4	0.1/0.1	0.0429
STU-T	0.06M	32	4	0.5/0.1	0.0688

Table 9: Ablation studies for Transformer Models

Transformer	0.07M	32	4	0.0/0.0	0.0472
Transformer	0.17M	64	4	0.0/0.0	0.0294
Transformer	0.30M	96	4	0.0/0.0	0.0214
Transformer	0.47M	128	4	0.0/0.0	0.0204
Transformer	0.02M	32	1	0.0/0.0	0.0545
Transformer	0.04M	32	2	0.0/0.0	0.0464
Transformer	0.07M	32	4	0.0/0.0	0.0472
Transformer	0.10M	32	6	0.0/0.0	0.0462
Transformer	0.07M	32	4	0.0/0.0	0.0472
Transformer	0.07M	32	4	0.1/0.1	0.0637
Transformer	0.07M	32	4	0.5/0.1	0.0961

Note that the noise level refers to the standard deviation of Gaussian noise added to the input data, while the frequency represents the probability of applying this noise to each data point. For example, 0.1/0.1 means that, on average, Gaussian noise with a standard deviation of 0.1 is applied to 10% of the data points.

E LLM experiments

Table 10: Model and Training Configuration Details for LLM Experiments

Model Architecture			
	Description	Flash STU	Transformer
Parameter Count	Total number of parameters	2,672M	2,667M
Embedding Dimension	Dimensionality of embedding space	1,536	1,536
Number of Heads	Attention heads (not multi-queried or multi-grouped)	8	8
Number of Layers	Transformer layers	26	25
ALiBi Attention	Attention scores modification using linear biases	Yes (interpolation factor: 0.25)	Yes (interpolation factor: 0.25)
Sliding Window Size	Sliding window attention context lookback size	1,024	8,192
Sequence Length (Training)	Input sequence length during training	8,192	8,192
Sequence Length (Inference)	Input sequence length during inference via position interpolation	32,768	32,768
Vocabulary Size	Size of the model’s vocabulary	200,064	200,064
MLP Expansion Factor	Expansion factor in MLP layers	12	12
Bias	Use of bias terms in linear layers	No	No
Dropout	Dropout rate	0.0	0.0
Number of Filters	Number of filters (Flash STU only)	24	–
Use Hankel_L	Alternative Hankel matrix (Flash STU only)	No	–
Learnable Filters	Learnable filters (Flash STU only)	Yes	–
Training and Optimization			
Epochs	Number of training epochs	1	1
Global Batch Size	Number of tokens processed per step	524,288	524,288
Micro Batch Size	Batch size per GPU	1	1
Gradient Accumulation Steps	Number of steps before performing a gradient update	8	8
Warmup Steps	Number of warmup steps	1,907	1,907
Evaluation Period	Evaluation frequency (steps)	25	25
Max Grad Norm	Maximum gradient norm for clipping	1.0	1.0
Optimizer Configuration			
Optimizer	Optimizer type	AdamW	AdamW
Learning Rate Schedule	LR scheduling strategy	Linear decay with warmup	Linear decay with warmup
Max Learning Rate	Maximum learning rate	3.0×10^{-4}	3.0×10^{-4}
Min Learning Rate	Minimum learning rate	3.0×10^{-5}	3.0×10^{-5}
Betas	Optimizer betas	(0.9, 0.999)	(0.9, 0.999)
Epsilon	Optimizer epsilon	1.0×10^{-8}	1.0×10^{-8}
Weight Decay	Weight decay factor	1.0×10^{-2}	1.0×10^{-2}
AMSGrad	Use AMSGrad variant	No	No
Fused	Use fused optimizer	Yes	Yes
Optimization Techniques			
Activation Checkpointing	Enable activation checkpointing	Yes	Yes
Use Flash FFT	Enable Flash FFT (Flash STU only)	Yes	–
Use TensorDot Approx.	Enable TensorDot approximation	Yes	–
Use Attention	Enable attention mechanism	Yes	Yes
Softcap	Softcap threshold	50.0	50.0
Torch Compile	Enable Torch compile optimization	No	No
Distributed Training Configuration			
FSDP	Fully Sharded Data Parallel	Yes	Yes
DDP	Distributed Data Parallel	No	No
Mixed Precision	Use mixed precision training	Yes	Yes
Torch Dtype	Data type for PyTorch tensors	bfloat16	bfloat16
CPU Offload	Offload computations to CPU	No	No
Sharding Strategy	Strategy for model sharding	Full Shard	Full Shard
FSDP Modules	Modules to apply FSDP	(STU, Attention, MLP)	(Attention, MLP)
State Dict Type	Type of state dictionary	Full	Full
Auto Wrap Policy	Policy for automatic wrapping	Partial	Partial
Backward Prefetch	Backward prefetch strategy	Backward Pre	Backward Pre
Forward Prefetch	Forward prefetch	No	No
Sync Module States	Synchronize module states across replicas	Yes	Yes
Use Original Params	Use original parameters during training	Yes	Yes

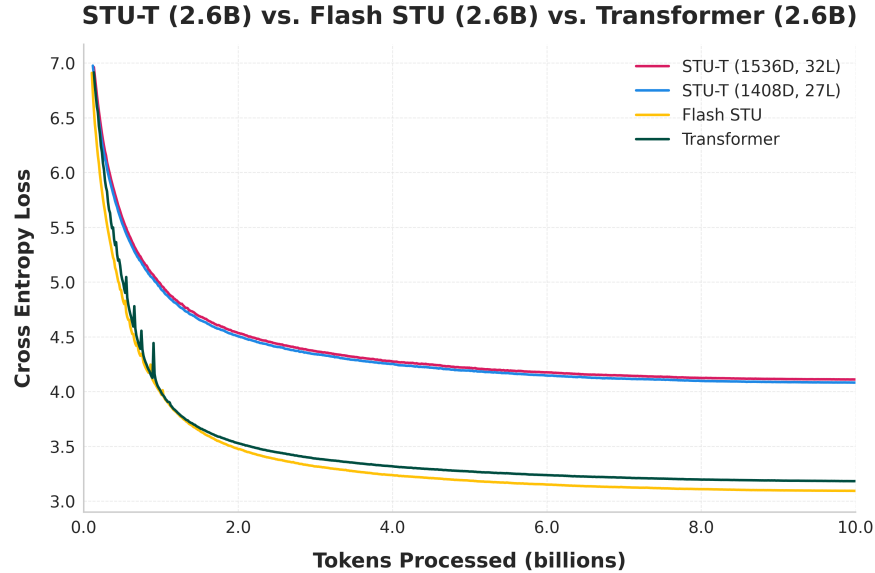


Figure 27: Comparison of STU-T, Flash STU, and Transformer on validation set

To further illustrate the capabilities of the Flash STU model, we present a sample output generated using a temperature of 1.0 and `top_k` sampling with $k = 50$:

Starter prompt: *"In a shocking finding, scientist discovered a herd of unicorns living in a remote, previously unexplored valley, in the Andes Mountains. Even more surprising to the researchers was the fact that the unicorns spoke perfect English."*

Generated output: *"In a shocking finding, scientist discovered a herd of unicorns living in a remote, previously unexplored valley, in the Andes Mountains. Even more surprising to the researchers was the fact that the unicorns spoke perfect English. Researchers now believe that these animals could now be a kind of hominid species.*

This discovery was recently made by scientists from the University of London. Previously, scientists had thought that this species stood only 5 feet (1.2 meters) for 15 minutes. But this new discovery was the first time a unicorn's eyes were ever revealed.

It was a perfect choice to do a lot of research on the species. In the end, to this day, we still can't say why the unicorns lived in this remote world - they were just another big black monkey. But the discovery proved that these unicorns used words and were able to communicate with other beings using the same words.

The study, which involved researchers from both Washington State University and Cornell University, confirmed that the unicorn family has existed for more than 10,000 years. It was also the first the species was studied and studied in its entirety.

'While there are also other rare wild animals like unicorns and hippopotami, most of these findings were not reported, but confirmed by numerous studies. In order to find their way out of an endangered species and find them, many endangered species require conservation programmes,' said lead researcher, Dr Thomas W. Huxley.

One of the key findings of the study in this week's issue is that the unicorns were able to walk forward and backward across the entire landscape. Their front limbs were able to reach all the way across the same landmass and in the same direction as their front legs were able to. These unique back limbs helped the animals to survive and thrive.

Other research has suggested that these unicorns have also been observed in the Andes Mountains. This is where the researchers believe they may have been able to find their way to the Andes. The area they found is the Amazon Valley.

The scientists believe that they came across an area that is part of the Amazon basin. In order to find out the true nature of this area, the researchers used satellite imagery from NASA for their research.

The scientists also believe that the unicorns might now also be found in other parts of the world, including North and South America. These discoveries might help scientists study an unknown area, such as the Amazonia and the Andes."